Journal of Power Sources 592 (2024) 233926



Contents lists available at ScienceDirect

Journal of Power Sources

journal homepage: www.elsevier.com/locate/jpowsour





Direct venting during fast charging of lithium-ion batteries

Yalun Li [a,b,**,1], Xinlei Gao [c,d,*,1], Huizhi Wang [c,d], Gregory J. Offer [c,d], Shichun Yang [e], Zhengming Zhao [a], Minggao Ouyang [b]

[a] Department of Electrical Engineering, Tsinghua University, Beijing, 100084, China
[b] School of Vehicle and Mobility, Tsinghua University, Beijing, 100084, China
[c] Department of Mechanical Engineering, Imperial College London, London, SW7 2AZ, United Kingdom
[d] The Faraday Institution, Harwell Science and Innovation Campus, Didcot, OX11 0RA, United Kingdom
[e] School of Transportation Science and Engineering, Beihang University, Beijing, China

HIGHLIGHTS

- Plated lithium with electrolyte can trigger early venting during thermal runaway.
- Side reactions cause consistent heat and gas generation during and after charging.
- Rapid gassing leads to direct venting after unreasonable fast charging.
- CO_2, CO and C_2H_4 account for most of the generated gases at early venting stage.

ARTICLE INFO

Keywords:
Lithium-ion battery
Fast charging
Lithium plating
Venting
Thermal runaway

ABSTRACT

Lithium-ion batteries pose high risks of failure when subjected to fast charging due to accumulated degradation from side reactions. Venting is a common failure behaviour that results in the release of gases and depressurization. However, the connection between fast-charging degradation and venting characteristics remains unclear. In this study, fast-charging experiments are conducted on $LiNi_{0.6}Mn_{0.2}Co_{0.2}O_2$ (NMC622)/graphite prismatic cells (51 Ah) with controlled cooling, followed by adiabatic thermal runaway tests. The degraded cell, after 4C charging, shows venting at a temperature 34.4 °C lower than a fresh cell. Gas analysis of the degraded anode-electrolyte partially reactive system in hot-box tests reveals that the reaction between plated lithium and electrolyte was a primary contributor to the additional gases. The fast-charging protocols are conducted under natural convection with less heat dissipation, causing battery swelling and venting without thermal runaway when subjected to excessive cycling at off-limit charge rates (5C and 5.6C). The temperature decreasing rates during rest after each charging process slow down or stabilize for a certain period, highlighting the role of exothermic side reactions. This experimentally demonstrates that venting failures can be directly triggered by the exothermic, gas generating reaction during fast charging. These findings inform future designs for safe and rapid battery charging.

1. Introduction

Fast charging of lithium-ion batteries (LIBs) is essential for reducing electric vehicle charging times and promoting road transport electrification [1,2]. However, fast charging leads to significant degradation, compromising the electrochemical performance of LIBs, including capacity and power output [3]. In extreme cases, fast charging can even compromise battery safety [4]. Hence, it is crucial to understand the impact of degradation caused by fast charging on battery safety.

The degradation of fast-charged LIBs has been extensively studied. Lithium (Li) plating has been identified as the dominant side reaction due to mismatched charge transfer with limited Li^+ intercalation during fast charging [5–8]. Tomaszewska et al. [6] provided an overview of fast charging physics as well as the associated degradation mechanisms and

* Corresponding author. Department of Mechanical Engineering, Imperial College London, London, SW7 2AZ, United Kingdom.
** Corresponding author. Department of Electrical Engineering, Tsinghua University, Beijing, 100084, China.
E-mail addresses: liyalun@tsinghua.edu.cn (Y. Li), x.gao22@imperial.ac.uk (X. Gao).
[1] These authors contributed equally to this work.

https://doi.org/10.1016/j.jpowsour.2023.233926
Received 17 September 2023; Received in revised form 9 November 2023; Accepted 3 December 2023
Available online 11 December 2023
0378-7753/© 2023 The Authors. Published by Elsevier B.V. This is an open access article under the CC BY license (http://creativecommons.org/licenses/by/4.0/).

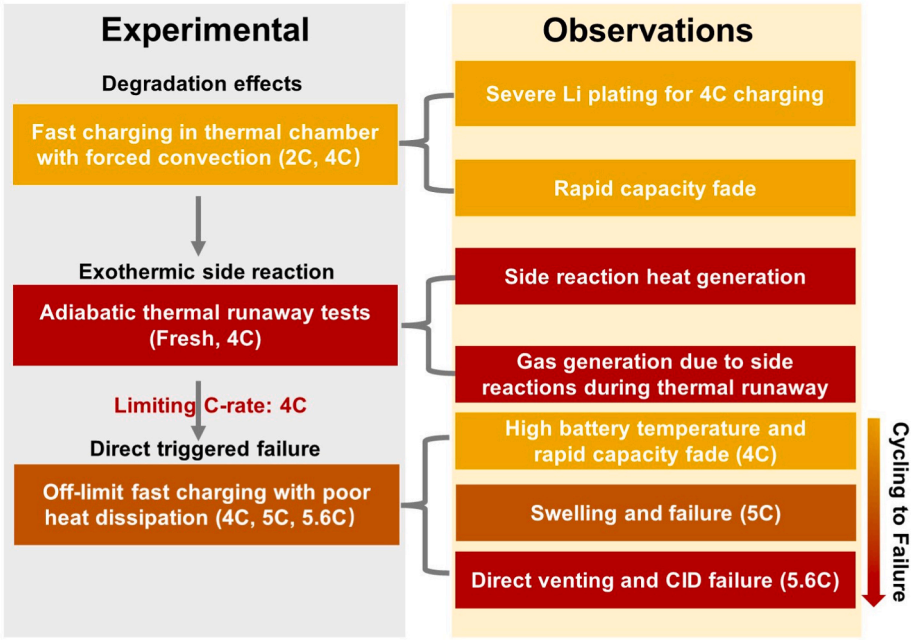


Fig. 1. Flow chart of the experiments and corresponding observations in this study.

mitigation strategies. The interplay between the primary and secondary degradation mechanisms was further reviewed by Edge et al. [9]. Despite the complex nature of battery degradation, key degradation mechanisms during fast charging can be identified using various characterization techniques. Xie et al. [3] conducted a cycle aging study on commercial 2.5 Ah 18650 cylindrical cells with $LiNi_{0.8}Co_{0.1}Mn_{0.1}O_2$ (NCM811) as cathodes and graphite as anodes. Post-mortem analyses showed that Li plating and solid electrolyte interphase (SEI) growth dominated the anode degradation, whereas secondary particle cracking and transition metal dissolution dominated the cathode degradation during fast-charge cycling. Mussa et al. [10] studied the ageing of a 25 Ah NCM/graphite prismatic cell under fast charging. They revealed that the cracking of NCM particles was not the dominant factor, while Li plating mainly accounts for the irreversible capacity loss under 3C charging. Besides, cell swelling was observed under 4C charging with the activation of current interruption device (CID). Chen et al. also reported in-operando optical observation of Li plating during high C-rate charging and proposed a strong correlation between incremental capacity (IC) peak with the onset of Li plating [11]. In addition, Xu and coworkers proposed a dynamic capacitance measurement method to detect Li plating in-operando based on the understanding of interfacial evolution along with Li plating, which facilitate the online diagnosis of fast charging degradation [12].

As an equally important metric to capacity and power, battery safety after fast charging has attracted growing attention [13–19]. Ren et al. [13] compared the thermal runaway (TR) behaviours of 24 Ah NCM111/graphite pouch cells under different aging conditions. Conventional characteristic temperatures in adiabatic TR tests in an accelerating rate calorimetry (ARC) were utilized to measure thermal stability. They found that the anode-electrolyte partial system with obvious Li plating substantially undermined the TR performance, while the cathode degradation only had negligible effects on battery safety. Li et al. [20] investigated the TR behaviours of NCM523/graphite pouch cells after fast charging. The cells after fast charging were found to have a shortened TR process with decreased self-heating and TR onset temperatures compared to fresh cells, which can be attributed to the reaction heat between plated Li and electrolyte. Another study by Li et al. [21] showed that the gas products from the reaction between plated Li and electrolyte led to an early eruption of pouch cells after fast charging. In addition, many abuse tests have been reported in the literature using various triggering methods such as overcharging, external heating and external short-circuit. There has been a consensus that cells after fast-charging degradation exhibit lower energy release but are easier to enter TR [22–24]. In addition, Waldman mentioned that the relaxation time after fast charging also has certain effects on TR behaviours, which can be associated with the re-intercalation of metallic Li into graphite anode [25]. Despite some changes in characteristic temperatures, the damage patterns of fast-charged cells with longer relaxation time are similar to those with shorter relaxation.

Less severe than TR, battery venting or CID activation is considered as moderate failure by which LIBs completely lose their functionality. Venting characteristics are also essential for assessing battery safety. Current studies on gassing mechanisms have mostly focused on overcharge and high-temperature cycling [26–33]. Michalak et al. [26] proposed that the electrochemical cross-talk can lead to gas evolution and capacity fade, which can be attributed to the SEI destruction process when anode potential increases above 0.9 V during discharging. Lu et al. [27] investigated the swelling mechanisms of a lithium iron phosphate battery under high-temperature storage with a state of charge (SOC) of 0%, and the SEI was found to decompose drastically at $> 50\ ^{\circ}C$ at high voltages, which facilitated the SEI reformation and gas generation. Wang et al. [29] performed high temperature 1C cycling tests on lithium titanate batteries at 55 °C, and their gas analysis showed that carbon dioxide (CO_2) and hydrogen (H_2) are the major gaseous products which can be attributed to water and solvent decomposition at high temperatures. Mattinen et al. [30] used on-line mass spectrometry to investigate gas evolution during cycling at different charge rates. Their results showed that the amount of ethylene (C_2H_4) gas was positively related to C-rates, and CO_2 and H_2 were reported to be the main gaseous species at high voltages (>4.15 V) and low voltages (<2.8 V). Aiming at Li plating, Gordon et al. reported a cycling protocol with high charge rate overcharge and high SOC window to induce Li plating as internal cell error and successfully trigger swelling and TR in different types of cells [33]. There lacks a systematic study on venting characteristics and gassing mechanisms during fast charging.

This study therefore focuses on battery venting during fast charging by addressing the following research questions: (1) How will the degradation induced by fast charging affect battery venting behaviours?

Table 1
Battery specifications.

Battery type	Prismatic
Operation Voltage (V)	2.8–4.2
Capacity (Ah)	51
Standard charge rate	0.33C
Maximum charge rate	2C
Energy density (Wh/kg)	204
Mass (g)	925
Cathode active material	NMC622
Anode active material	Graphite
Electrolyte	$LiPF_6$/EC, DMC, EMC
Separator	Polyethylene (PE)/Ceramic

(2) What are the major side reactions responsible for the rapid internal pressure build-up during fast charging? (3) What operating conditions can trigger venting during fast charging? A series of experiments were designed with a flowchart illustrated in Fig. 1. Fast-charge cycling experiments at different C-rates under controlled cooling were first conducted to study the electrochemical-thermal characteristics and degradation mechanisms during fast charging as well as to identify the limiting C-rate can cause observable effects on battery venting behaviours in terms of thermal safety during TR tests. The fast-charge cycling experiments were followed by adiabatic TR tests and hot-box tests with gas analysis to study the effects of fast-charging degradation on TR and venting behaviours. To investigate how heat removal rate will affect fast-charge degradation and battery safety failure behaviours, the fast-charge cycling tests were conducted under forced and natural convection conditions. Based on the findings from the fast-charge cycling and TR experiments, off-limit charging tests were designed, which successfully triggered non-TR venting failure during fast charging. Post-mortem analyses were conducted after the off-limit charging tests. The study provides valuable insights into battery venting caused by fast charging, informing future designs for safe and rapid battery charging.

2. Experimental

2.1. Fast charging and excessive cycling tests

The batteries used in this study are 51 Ah commercial prismatic batteries with NCM622 and graphite as cathode and anode active materials respectively. Lithium hexafluorophosphate ($LiPF_6$) solution in ethylene carbonate (EC), dimethyl carbonate (DMC), and ethyl methyl carbonate is used as the electrolyte. Specifications of the prismatic battery were summarized in Table 1. The standard and maximum charge rates recommended by the battery manufacturer are 0.33C and 2C, respectively. Hence, charging at C-rates $>$ 2C can be considered as fast charging. This prismatic battery is equipped with passive protection designs including a CID and venting valve to cut off the current and release the gases inside the battery when the internal pressure exceeds a certain safety threshold. The fresh batteries were first operated with capacity check-up procedures including three cycles of 1/3C constant current constant voltage (CC-CV) charging and 1C constant current (CC) discharging. Each charging and discharging process was followed by a 1-h rest period to stabilize the batteries. Then, the batteries were cycled with CC fast charging at different C-rates (1C, 2C and 4C) to 4.2 V and 1C CC discharging to 2.8 V. The capacity check-up produces were performed every 10 fast-charge cycles to record the capacity retention. Cycling was terminated when the checked capacity retention dropped below 80% for 4C charged cell, which is a common indicator for capacity failure. Note that the rest period after fast charging was also performed with differential voltage analyses to identify the degradation mechanisms. All these tests were conducted in forced convection thermal chambers at 25 °C with voltage and cell surface temperature recorded at the time interval of 1 s throughout the tests using NEWARE battery cycler (CT-8004-5V200Q-NTFA). Additional fast-charge cycling tests at 4C, 5C and 5.6C were conducted in thermal chambers under natural convection using Arbin's battery cycler (Laboratory Battery Test Series, maximum current $<$ 300 A) to study the effects of cooling conditions and deliberately trigger venting failure. Images were taken 2 h after the end of rest period, and then post-mortem analyses were performed accordingly after the cell cooled down for one day.

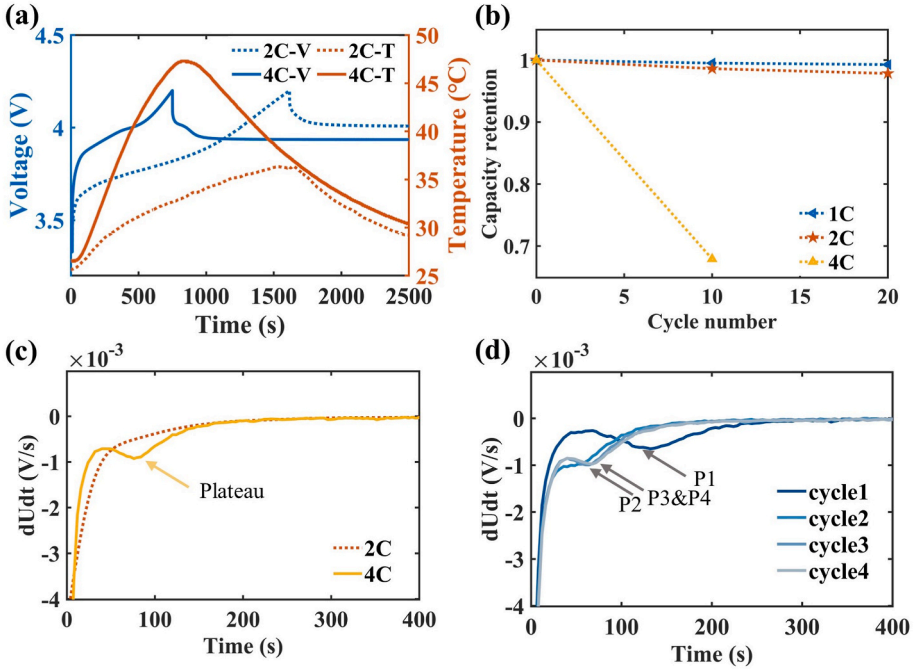


Fig. 2. Electrochemical-thermal characteristics during fast-charge cycling under forced convection: (a) voltage and average temperature profiles for the 1st charging-rest period at different C-rates, (b) charge capacity versus cycle number at different C-rates, (c) differential voltages during rest after the 1st charging at different C-rates, and (d) differential voltages after cycle numbers from 1 to 4 at a 4C charge rate.

2.2. ARC tests

The adiabatic TR tests were performed with fresh and fast-charged batteries in an Extended-Volume ARC (EV + ARC) produced by Thermal Hazard Technology. All TR tests for the fast-charged batteries were conducted within 1 h after the 2nd fast-charge cycle. In the TR tests, the batteries were placed at the bottom centre of the ARC chamber with the voltage and temperature recorded at a time interval of 1 s. The heat-wait-seek (HWS) mode was operated for the ARC before switching to the adiabatic mode with the procedures detailed elsewhere [34]. Adiabatic environments were simulated in the ARC chamber to fully capture the heat generation without any heat dissipation. Therefore, any exothermic reactions can be identified by characterizing the peaks in temperature rise rate curves. In addition, the sudden drop of temperature rise rate curve can be used to indicate the occurrence of battery venting due to the sudden energy release through the venting valve [35].

2.3. Hot-box tests and post-mortem analyses

Partially reactive systems were used to separate a full battery cell into anode-electrolyte, cathode-electrolyte, or cathode-anode systems for further analyses with experimental procedures detailed in our previous study [21]. After the capacity check-up, a battery after 10 cycles of 4C fast-charge cycling under forced convection was dissembled in an argon-filled glove box. The degraded anode was taken out of the jellyroll and soaked in DMC to wash off the residual electrolyte. After 24 h of storage in the glove box, the anode powders were scratched off the current collector. The dry powders were then loaded into an aluminium plastic bag with a volume of 1.2 L. The same electrolyte (1 M $LiPF_6$ in EC-DMC-EMC) was added into the bag following the same mass ratio of anode to electrolyte as the full cell detailed in our previous study [21]. After sealing the aluminium plastic bag with the anode-electrolyte mixture, the partially reactive system was placed into a hot-box and gradually heated up to 120 °C. The bag underwent massive expansion due to rapid gas generation and pressure build-up. After cooling down the hot-box, the bag shrank because of condensation of electrolyte vapor and the remaining gases were collected and analysed using gas chromatography. As for those batteries cycled under natural convection, they were dissembled in a glove box after any of failure events such as low capacity retention, swelling and venting occurred. It is noted that the jellyroll of the 4C battery under natural convection was resealed in an aluminium plastic bag and put under storage for one month before further gas analyses, whereas the 5C and 5.6C batteries under natural convection were disposed immediately after disassembly for safety reasons.

3. Results and discussion

3.1. Capacity fade and Li plating

Fig. 2 shows the electrochemical-thermal characteristics during fast-charge cycling. Since the tests were conducted in thermal chambers with a constant temperature of 25 °C under forced convection, the battery temperature remained within 50 °C even for 4C charging. For the first cycle, charge capacities of 44.06 Ah and 41.59 Ah were respectively obtained at 2C and 4C before reaching the cut-off voltage of 4.2 V. Fig. 2 (a) shows that the 4C-charged battery gave a higher peak temperature (47 °C) compared to the 2C-charged battery (36 °C) due to the larger heat generation at a higher C-rate. Fig. 2(b) shows accelerated capacity fade for check-up points at a higher C-rate. The capacity retention dropped to 67.3% after 10 cycles for 4C fast-charge cycling, while 2C cycling only caused 2.1% of capacity fade after 20 cycles. Additional 1C cycling for the same number of cycles to 20 cycles were conducted, which only caused 0.003% of capacity loss, showing negligible degradation within 20 cycles. As shown in Figs. S1(a) and (b), the discharge capacity during cycling also decreased with a higher C-rate, and 4C

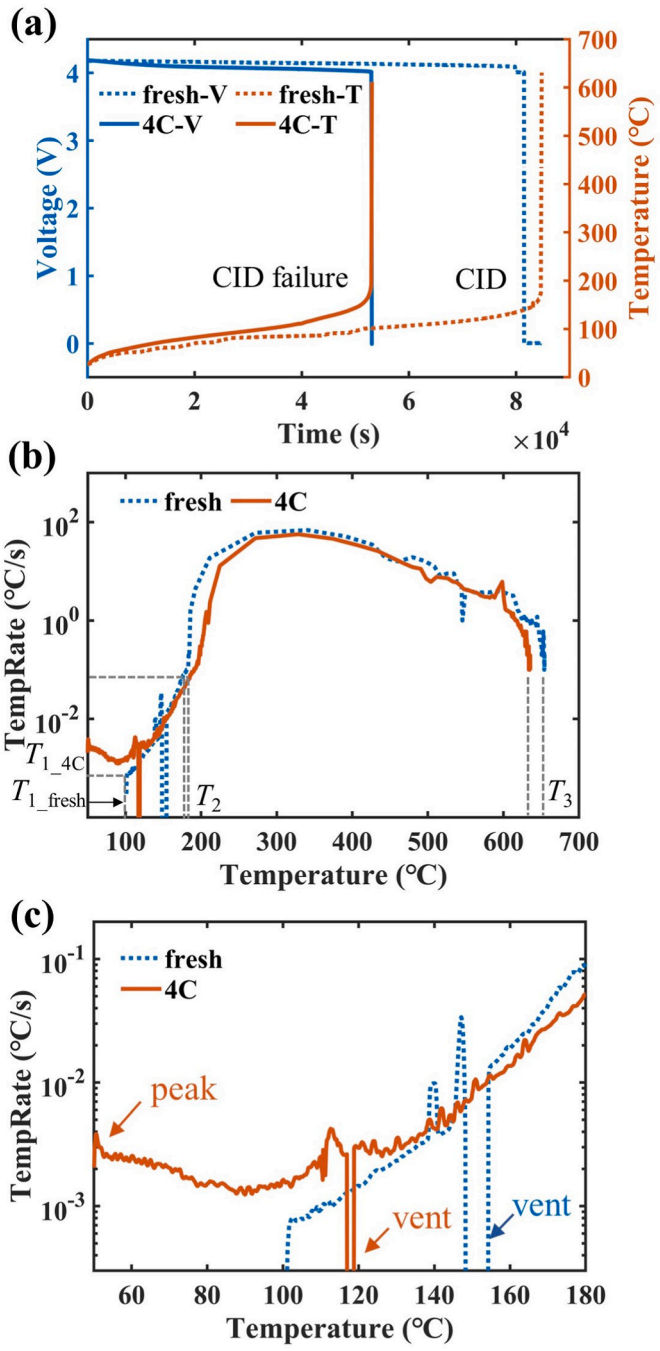


Fig. 3. Adiabatic TR tests for fresh and 4C fast charged (after the 2nd cycle) cells. (a) Temperature and voltage changes versus time; (b) Temperature rise rate versus temperature (b1) with an enlarged view for temperatures <180 °C (b2).

cycling showed a tremendous drop in discharge capacity from 39.3 Ah to 17.5 Ah. Fig. S2 shows the incremental capacity curves of fresh, 1C, 2C and 4C cells, respectively. Compared to fresh cells, 1C and 2C charged cells show similar IC curves of 0.05C discharge, indicating no obvious LAM or LLI occurred for 1C and 2C charged cell, while 4C charged cell shows weakened and shifted peaks due to massive degradation compared to 1C and 2C cells, which is consistent with poor capacity retention of 67.3% after 10 cycles of 4C fast-charge.

The capacity fade increase with increasing C-rate was further examined with differential voltage during rest after charging process, which is commonly utilized as auxiliary evidence for Li plating/

Table 2
Characteristic temperatures and failure events during adiabatic TR tests.

	Fresh	after 4C charging
Self-heating temperature, T_1 (°C)	101	50
Temperature at which CID activated, T_{CID} (°C)	139.3	–
Venting temperature, T_{vent} (°C)	152.4	118
TR triggering temperature, T_2 (°C)	185.9	197.3
Maximum temperature, T_3 (°C)	654.8	635.3

stripping [36–38]. Although some may argue that absence of voltage plateau does not mean the absence of Li plating, the rest voltage plateau evidence can still be valid because capacity fade under 2C was negligible compared to that under 4C. To rule out the possibility of unobservable Li plating under 2C, scanning electron microscopy (SEM) images of fresh cell and 2C-charged cell are shown in Fig. S3 and Fig. S4, respectively. Comparing to the fresh cell, the 2C-charged cell showed no obvious change in surface morphology for both anode and cathode sides, confirming that Li plating can be negligible in degradation analysis under 2C charging under forced convection. In the meantime, 4C cycling led to an obvious voltage plateau whereas 2C cycling led to no plateau, as shown in Fig. 2(c), indicating the occurrence of Li plating under 4C charging. To study the amount of plated Li during 4C cycling, differential voltages after cycle numbers from 1 to 4 are compared in Fig. 2(d). It can be observed that the first rest stage exhibited a later voltage plateau while the following three cycles exhibited similar voltage plateaus. This is consistent with the findings in the literature which showed the first cycle produced a larger amount of plated Li [38]. The analyses above confirm that Li plating dominated the rapid capacity fade during fast-charge cycling at 4C.

3.2. TR and gassing characteristics after fast charging

TR characteristics of fresh and 4C fast-charged batteries are compared in Fig. 3. The 4C fast charging under room temperature is selected for comparisons and for the analyses in the rest of the paper because 4C was identified as the limiting C-rate that can trigger observable effects on venting behaviours in terms of thermal safety as detailed in the Supplementary Information. The characteristic temperatures and failure events during the adiabatic TR tests are summarized in Table 2. In Fig. 3(a), the fast-charged battery gives a shorter TR process than the fresh battery. TR test results for a 3C-charged battery and the corresponding features are given in Table S1 and Fig. S5 in the Supplementary Information. It also can be found that the fast-charged battery experienced earlier self-heating compared to the fresh battery, with self-heating temperatures (T_1) of 62 °C and 50 °C, respectively. This can be mainly attributed to the exothermic reaction between the plated Li and electrolyte. In contrast, the triggering temperature (T_2) and the maximum temperature (T_3) of the fast charged batteries are close or only slightly higher than those of the fresh battery as shown in Table 2. Although the fast-charged battery has accumulated a certain amount of plated Li after 2 cycles of fast charging, the degradation was not comparable to a typical fast charging aging study which can last for months. Therefore, the total energy released during TR of the fast-charged battery showed a slight difference from that of the fresh battery. The CID was successfully activated for the fresh battery, resulting in an immediate voltage drop to 0 V and a temporary pause in the temperature rise. However, the CID failed to be activated for the fast-charged battery. Fig. 3(b) shows the temperature rise rate during the TR tests, which increased slowly until reaching T_2 and rapidly increased to the maximum temperature rise rate before cooling down. The enlarged figure shown in the inset of Fig. 3(c) indicates that venting occurred for both the fresh and fast-charged batteries. The fast-charged battery showed much earlier venting at a temperature of 118 °C compared to the fresh battery (which exhibited a venting temperature of 152.4 °C). Fast charging process promotes Li plating and releases some additional gases along with Li plating, both the heat and additional gases can increase the

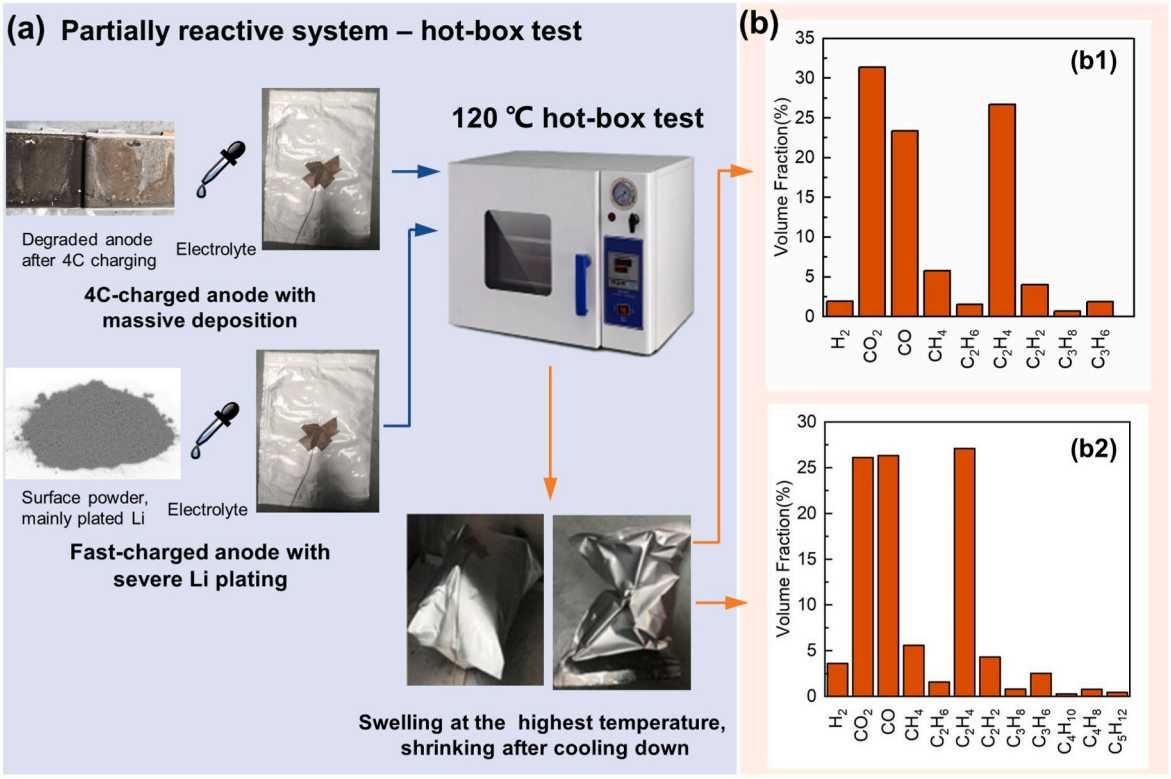


Fig. 4. Gas analysis of 120 °C hot-box tests for anode-electrolyte partially reactive system after 4C fast charging. (a) Preparation of hot-box tests; (b) Gas compositions of 4C-charged anode with electrolyte (this study, b1) and fast-charged anode (surface layer powder, mainly plated Li, b2) with electrolyte [21].

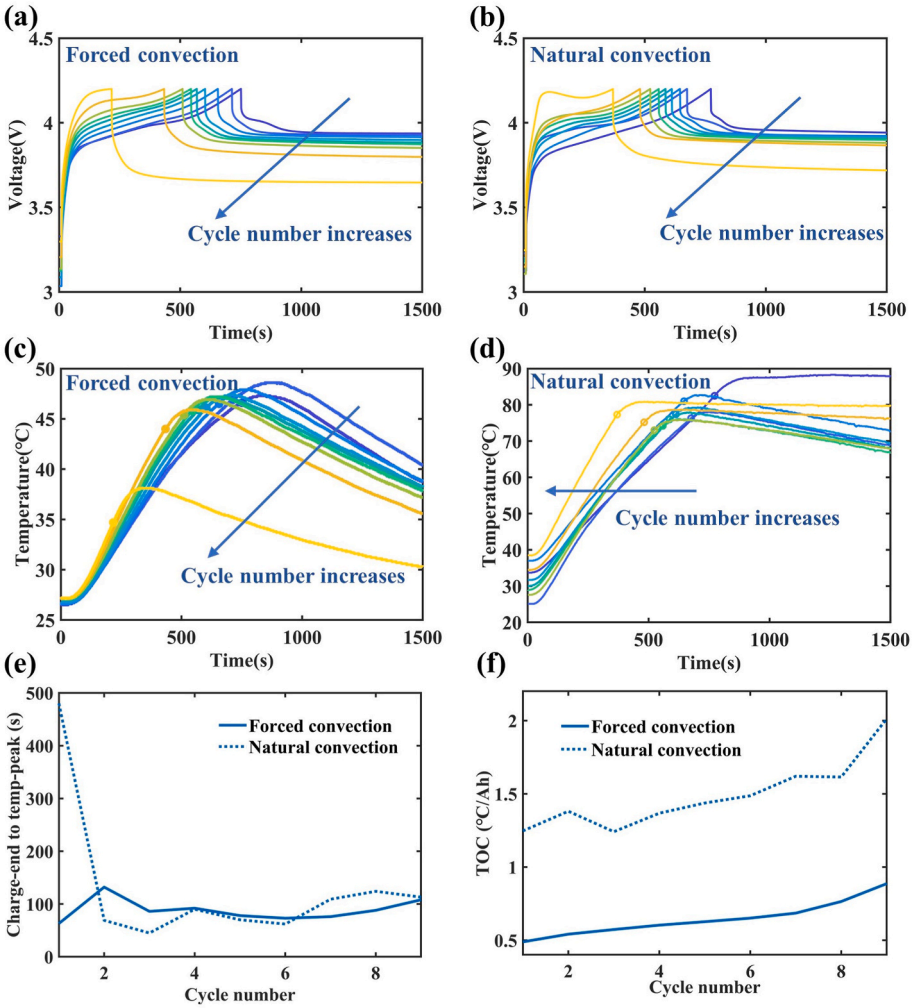


Fig. 5. Voltage and temperature profiles during fast charging under different cooling conditions. 4C charging voltages for 9 cycles under (a) forced and (b) natural convection. 4C charging temperatures for 9 cycles under (c) forced and (d) natural convection. (e) Interval from charge-end to temperature-peak and (f) TOC versus cycle number under forced and natural convection.

internal pressure during fast charging. But when the cell cools down, thermal expansion can be neglected, the remaining gases inside the battery will maintain the internal pressure at a certain level which is potentially not high enough to trigger battery venting directly. However, when the battery cell was abused, more gases are generated from the decomposition reactions. Hence the battery will potentially go through an earlier venting when abused with certain pressure level accumulated from fast charging process. Additionally, the plated Li from the same fast charging has shown to react with electrolyte with elevated temperature, which is another gas source that contributes to total pressure build-up during abuse tests. Interestingly, the fast-charged battery exhibited an extra exothermic peak below 60 °C, which was due to the reaction of the plated Li with electrolyte and fell within the temperature range for fast charging. This can compromise safety performance during fast-charge cycling because of the considerable heat generation and gas evolution as a result of the exothermic side reaction.

As the ARC test showed that venting occurred at 118 °C for the 4C fast-charged battery, 120 °C hot-box tests for the anode-electrolyte partially reactive system were conducted to identify the composition of the vented gas as described in Fig. 4(a). Fig. 4(b1) shows the gas composition of the anode-electrolyte partially reactive system acquired from the 4C-charged battery. CO_2, C_2H_4 and carbon monoxide (CO) account for the majority of the generated gas with volume fractions of 31.4%, 26.7% and 23.4%, respectively. The main gas sources include the SEI decomposition, the reaction between the plated Li and electrolyte as well as the reaction between the intercalated Li within the anode and electrolyte [21,29,39]. The gas composition in this study is similar to that obtained from a 120 °C hot-box test in our previous study where surface powders of a highly degraded anode (mostly plated Li) was mixed with the electrolyte (Fig. 4(b2)) [9]. This also indicates that metallic Li was plated on the anode surface for the fast-charged battery at 4C, and the exothermic reaction between the plated Li and electrolyte produced the extra gas contributing to the earlier pressure build-up compared to a fresh battery.

3.3. Fast-charge cycling under different cooling conditions

The ARC test results indicate that the plated Li induced by fast-charge cycling can compromise battery safety under 60 °C even with sufficient cooling. To emphasize the importance of sufficient cooling in preventing battery safety failure especially under fast-charge scenarios, two different cooling conditions, forced convection and natural convection, were applied for fast-charge cycling at 4C to study the effect of heat removal rate on fast-charging safety. Fig. 5(a)-(d) show the voltage and temperature profiles of the fast-charging process for 9 cycles under the two different cooling conditions. The 10th cycle could not be finished because of a sudden capacity drop and highly misshaped voltage for both cooling conditions. The charge capacity during the CC stage under forced convection dropped from 41.1 Ah to 11.4 Ah, whereas that under natural convection dropped from 43.2 Ah to 29.1

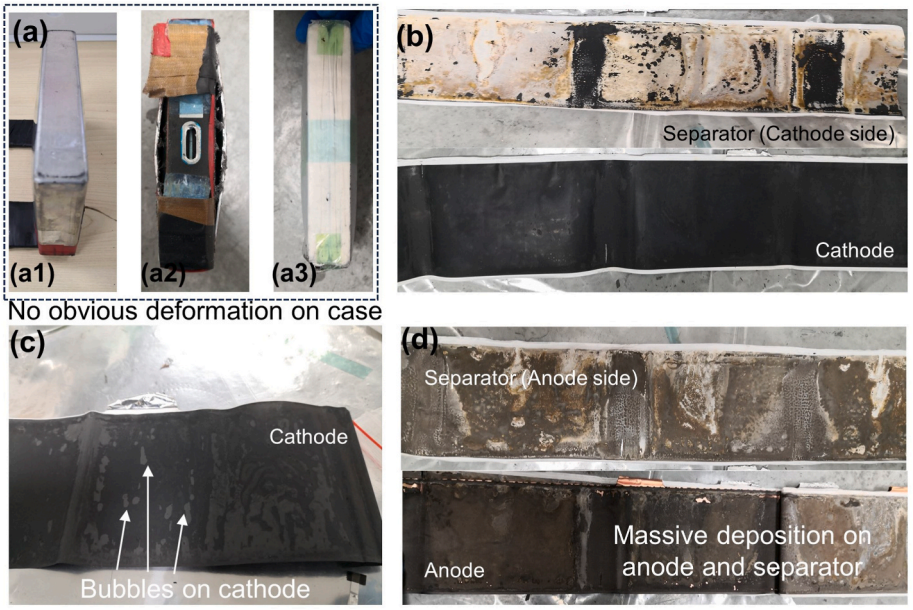


Fig. 6. Disassembly of the battery charged at 4C under natural convection. (a) Battery case and jellyroll; (b) Cathode and separator (cathode side); (c) Expansion of cathode with bubble-like defects; (d) Anode and separator (anode side).

Ah. This agrees with the findings in other studies [40,41] that higher temperatures are favoured by fast charging as higher temperatures can alleviate Li plating and thus capacity fade. However, the voltage curves under natural convection (Fig. 5(b)) tended to misshape and even exhibited a voltage valley during the charge process of the 9th cycle, while the voltage curves under forced convection did not show this variation trend. A possible reason is the sudden internal resistance drop due to the higher cell temperature induced by fast charging under natural convection. It also can be seen that differential voltage plateau during rest period only appeared for the first few cycles, indicating more plated Li were accumulated during those cycles (Fig. S6, Supplementary Information).

The corresponding temperature profiles under forced and natural convection are respectively shown in Fig. 5(b) and (d). Table S2 shows temperature rise during the 1st charging process at different C-rates and cooling conditions. It is noticeable that with 4C charging under forced convection, a temperature rise of 20.1 °C was obtained, while 1C charging only led to 1 °C of temperature rise. Key data points of the temperature profiles with C-rate of 4C are listed in Table S3 and Table S4 in the Supplementary Information. Due to less heat dissipation, natural convection yielded higher temperatures than forced convection. The maximum temperature during fast-charge cycling under natural convection reached up to 88.3 °C in the first cycle and decreased to 80.7 °C in the last cycle. Under forced convection, the maximum temperatures in the first and last cycles were 48.8 °C–38.1 °C, respectively. Interestingly, the maximum temperature appeared after the end of each fast-charging process for all cycles under both cooling conditions. Based on the analyses in previous sections, the exothermic reaction between the plated Li and electrolyte was preferably triggered under 60 °C, therefore, it can contribute to heat generation even during rest after charging. This can be further proved by the temperature change during rest for the battery under natural convection in Fig. 5(d). The rate of temperature decrease was slowed with continuous heat generation and dissipation, and the temperature remained around the maximum value during rest for the last two cycles.

To assess the heat-generation contribution of the reaction between the plated Li and electrolyte, time intervals from charge-end to temperature-peak of each cycle and a parameter, TOC (TempOver-Charge), defined as the maximum temperature rise divided by charge capacity (TOC = $\Delta T_{max}/Q_{charge}$) are plotted in Fig. 5(e) and (f), respectively. The time interval serves as an indicator of the intensity of exothermic side reactions following the charging process. Meanwhile, TOC reflects the average temperature increase associated with the input of 1 Ah of capacity into the battery, also indicating the heat contribution from side reactions during charging. In conditions of forced convection, the peak temperature typically manifested approximately 100 s after charging, with TOC values observed to gradually rise from 0.49 to 0.89, as depicted in Fig. 5(f). This observation suggests that the ongoing reaction between the plated lithium and the electrolyte continued to produce heat subsequent to the charging phase, with the heat contribution from side reactions showing an increasing trend alongside the progressive accumulation of degradation. In contrast, under natural convection where heat dissipation is less efficient, cell temperatures were noted to reach as high as 90 °C, undeniably exacerbating the exothermic reactions. Since it has been reported in the literature that the reaction of metallic Li with electrolyte can be quite active at ~100 °C [20,21], the Li-electrolyte reaction can become more active at high temperatures despite less plated Li accumulated. The maximum temperature occurred at 400 s later than the end of charging at the first cycle, indicating a continuous and fierce reaction heat when the plated Li was firstly generated and consumed at 80 °C. Compared to forced convection, the TOC under natural convection had higher values ranging from 1.25 to 2 but exhibited a similar variation trend. Therefore, it can be preliminarily concluded that the contribution of the side reaction heat kept increasing as degradation accumulated until the battery capacity dropped below the failure point of state of health. Regarding the difference between normal and fast charging, no temperature peak delay can be found in 1C and 2C charged cell as opposed to 4C fast-charged cell. In addition, corresponding TOC curves versus cycle number under different C-rates are shown in Fig. S7. Cells under relatively low C-rates exhibit consistent TOC thermal behaviours instead of increasing, which can be attributed to less degradation under low C-rates. TOC values for 1C and 2C charged cycles under forced convection are 0.015 and 0.25 respectively, which are much lower than that under 4C fast-charged cell, indicating limited heat accumulation during charge process and negligible heat contribution from side reactions.

Fig. 6 presents images of a 4C fast-charged battery, post-disassembly, elucidating the effects of fast charging under natural convection on its structural integrity and surface morphology. As shown in Fig. 6(a1) and (a2), there was observable yet moderate deformation on the battery

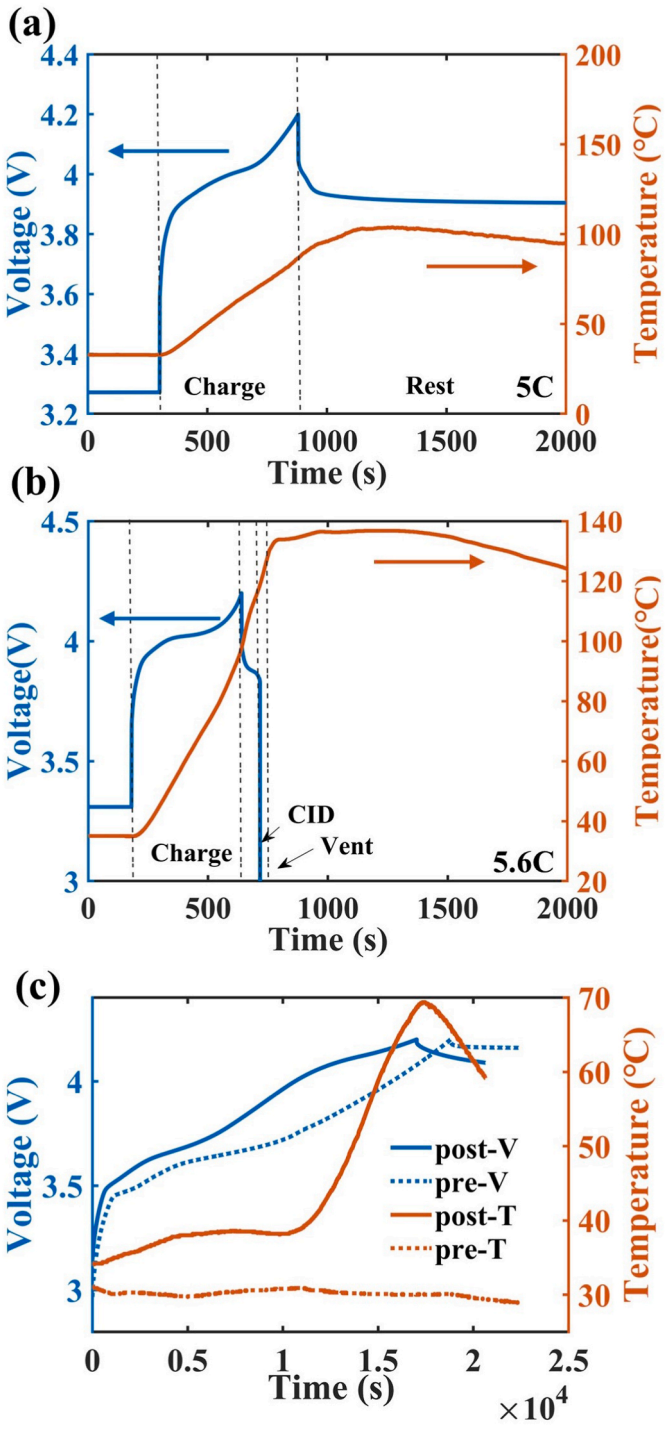


Fig. 7. Voltage and temperature profiles during the 1st cycle for off-limit fast charging at (a) 5C and (b) 5.6C under natural convection; (b) Comparisons of voltage and temperature under 0.2C charging between fresh and post-5C batteries.

casing, indicating that the gases generated from the exothermic reactions under this circumstance were insufficient in magnitude to exert enough internal pressure that would result in extensive swelling of the battery. And the jellyroll remained intact from the bottom view according to Fig. 6(a3) despite of some minor swelling. In contrast, Fig. 6 (b) and (c) reveal more pronounced internal damage. Here, bubble-like defects and delamination can be observed on the cathode surface and the cathode side of the separator, which can account for less utilization of cathode and loss of active materials. However, according to the SEM images of the cathode side after disassembly (Figs. S8(c) and (d)), no obvious particle cracking or morphology change can be found. Additionally, cathode samples were taken from the disassembled jellyroll with 0 SOC of locations as shown in Fig. S9, and the corresponding cathode potentials versus Li/Li^+ are shown in Table S5. Compared to the fully-lithiated fresh cathode potential of 3.02 V, the aged cathode showed a much higher potential from 3.55 V to 3.77 V, indicating severe over-lithiation for cathode after 10 cycles of 4C fast-charge cycling under natural convection. Location #2 and #5 gave higher potentials of 3.75 V and 3.77 V among all the locations, showing potential inhomogeneity with more electrode damage around the centre of cathode.

Additionally, a substantial accumulation of mud-like deposits is visible on the anode surface and its side of the separator. This degradation can be ascribed to a combination of severe Li plating, SEI decomposition, and electrolyte dry-out. Figs. S8(c) and (d) further show the surface morphology from the anode side, and massive plated Li was observed after 4C-charge cycling, covering all round the anode particles. Therefore, these observations confirmed that the internal structures of the battery have undergone significant damage, which can be predominantly attributed to the fast-charge cycling and elevated temperature conditions.

3.4. Fast charge cycling to venting

Poor heat removal rate will jeopardize battery safety by promoting the exothermic and gas-releasing reaction between plated Li with electrolyte within favourable temperature range from 60 °C to 120 °C. In order to investigate what conditions can directly trigger battery safety failure. We further increased the C-rate to 5C under natural convection to deliberately trigger failure during cycling. Fig. 7 (a) show the voltage and temperature profiles of the first cycle at 5C. It can be seen in the figure that CC charging lasted for 579 s until the cut-off voltage of 4.2 V was reached and a total capacity of 40.1 Ah was charged to the battery. As shown in Fig. S10, the differential voltage plateau during the following rest period indicated the occurrence of Li plating. The temperature reached its maximum value at $>$ 100 °C at around 300 s after the end of charging. Battery swelling was also observed for this cell due to high internal pressure built-up as a result of more gas generation from side reactions according to Fig. 8 (a). After one cycle of 5C charging, the battery could not be charged under a normal C-rate due to severe degradation. Fig. 7 (c) compares the voltage and temperature profiles of the battery after 5C charging with a fresh battery under 0.2C charging. The voltage after 5C charging was misshaped with less chargeable capacity. Due to the relatively low C-rate of 0.2C, the voltage curve roughly reflected the pseudo-open circuit voltage, apparently, the battery was damaged after the off-limit fast charging. Regarding the thermal characteristics, the 0.2C charging to the fresh battery generated little heat, while the post-5C battery exhibited an abnormally high temperature rise up to 70 °C at the later stage during charging. This phenomenon can be caused by the combination of increased polarization heat and residual heat resulting from the exothermic side reaction between plated Li with electrolyte even after the end of fast charging.

The C-rate was further increased to 5.6C to explore the safety limit of the battery as shown in Fig. 7(b). The charging was cut off at 4.2 V after 460 s as expected with an end-of-charge temperature of 96 °C. Under 5.6C fast charging, the internal pressure exceeded both the thresholds for the CID and safety valve activation. During the rest period, the temperature of battery continued to climb up to 119 °C after 78 s when the CID was activated due to rapid gas generation and the voltage dropped to 0 V. The safety valve was also activated 36 s later than the CID activation with obvious noise and fierce venting. After that, the temperature continued to increase to 140 °C, which is almost 40 °C higher than the self-heating temperature of the fresh battery in ARC tests. Due to the passive protection designs of the CID and venting valve, the temperature of the 5.6C battery did not continue to rise so that irreversible TR was not triggered. However, the battery remained in

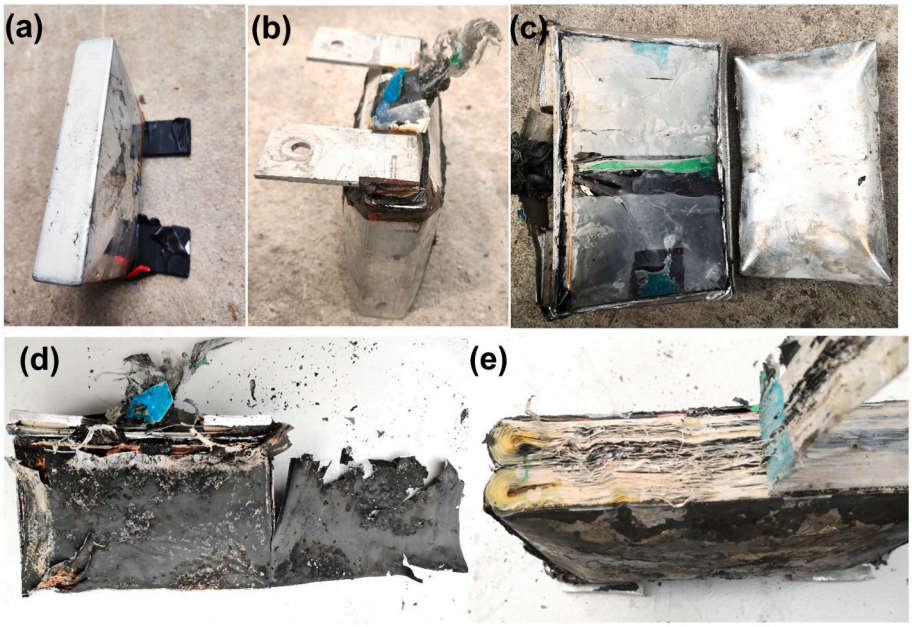


Fig. 8. Disassembly of the 5C and 5.6C charged batteries. Battery cases after (a) 5C and (b) 5.6C charging; (c) Opened battery case after 5.6C charging; (d) Melting of the outer insulation film of the jellyroll and delaminated active material after 5.6C; (e) Opened jellyroll of the 5.6C battery.

unstable status and could be considered as failure. In this test, direct venting failure was successfully triggered by off-limit fast charging with poor heat dissipation, which can happen in real-life applications if a battery exceeds a certain charge rate with insufficient thermal management. In this study, with dynamic pressure build-up and rapid temperature rise rate caused by fast charging, a relatively low venting temperature of 119 °C was obtained during the off-limit charging tests, which further confirmed that there were additional gases generated before venting below 120 °C. This is also consistent with our findings that plated Li can react with electrolyte and produce additional gases even during fast charging. Regarding the gas generation from cathode, NMC cathode can release oxygen when the layered structure begins to decompose with elevated temperatures, which can promote further heat and gas generation. However, according to some relevant studies [42–45], the thermal decomposition temperature range of cathode during TR is generally above 150–200 °C, before that the cathode remains stable while the main gas and heat sources come from the reactions of anode side, including SEI decomposition, the reaction between intercalated Li with electrolyte as well as the reaction between plated Li with electrolyte. Hence, the gas generation from cathode side can be negligible compared to that from anode side in this study.

Fig. 8(a) and (b) show the images of the 5C and 5.6C batteries after swelling and venting, respectively. Both battery cases swelled up, and small part of jellyroll of the 5.6C battery was pushed out of safety valve due to severe venting. Images taken after the removal of the battery case are shown in Fig. 8(c) and (d). The jellyroll deformed significantly due to the gas accumulation between the layers. In Fig. 8(d), distinct delamination of the active materials on the electrodes and the occurrence of melting in the outer insulation film can be observed, suggesting massive loss of active materials induced by 5.6C charging. Fig. 8(e) shows the bottom view of the opened jellyroll, and the inner structure was distorted due to the severe degradation. Therefore, it can be concluded that fast charging can cause considerable damage to battery internal structures and even directly induce venting in a non-adiabatic environment. In a sense, passive protection design of safety valve plays an essential role in delaying TR especially under fast charging conditions.

4. Conclusions

This study conducted a series of experiments to investigate fast-charging degradation effects on battery safety especially venting characteristics. Main degradation mechanisms during fast-charge cycling were identified and their effects on safety behaviours were discussed. The operating conditions that can trigger battery venting during fast charging were demonstrated.

The results demonstrated significant capacity fade of over 30% in the battery after 10 cycles of 4C fast charging and 1C discharging under forced convection, whereas 2C charged batteries exhibited negligible capacity fade. Li plating/stripping was evidenced by differential voltage plateaus during rest post-fast charging. Adiabatic TR tests revealed that 4C fast charging compromised battery safety, reducing the onset temperatures for both self-heating and venting, and introduced extra exothermic reactions between plated Li and electrolyte below 60 °C. Early venting of the 4C charged battery during the TR test indicated that the extra exothermic reaction not only contributed to heat generation but also gas generation.

Comparative studies under different cooling conditions showed that the 4C-charged battery under natural convection experienced higher heat accumulation from side reactions during fast charging, peaking at over 80 °C and maintaining high temperatures even after charging process, indicating additional exothermic side reactions and insufficient heat dissipation. Disassembly and gas analysis further verified Li plating and the reaction between plated Li and electrolyte, identifying CO, CO_2, and C_2H_4 as primary gases produced during early venting.

Battery swelling and venting were triggered under fast charging at 5C and 5.6C under natural convection. However, TR was prevented due to the activation of the CID and venting valve, highlighting the importance of the passive protection designs. This study experimentally demonstrated that venting failure can be directly triggered by the exothermic, gas generating reaction between plated lithium and electrolyte during fast charging. These findings provide valuable insights into battery venting caused by fast charging, informing future designs for safe and rapid battery charging.

CRediT authorship contribution statement

Yalun Li: Conceptualization, Investigation, Data curation, Writing – review & editing, Funding acquisition. **Xinlei Gao:** Methodology, Investigation, Data curation, Writing – original draft, Writing – review & editing. **Huizhi Wang:** Writing – review & editing. **Gregory J. Offer:** Writing – review & editing. **Shichun Yang:** Writing – review & editing. **Zhengming Zhao:** Writing – review & editing. **Minggao Ouyang:** Writing – review & editing.

Declaration of competing interest

The authors declare that they have no known competing financial interests or personal relationships that could have appeared to influence the work reported in this paper.

Data availability

Data will be made available on request.

Acknowledgements

This work is supported by the National Natural Science Foundation of China (Grant No. 52207241), China National Postdoctoral Program for Innovative Talents (Grant No. BX20220171), China Postdoctoral Science Foundation (Grant No. 2022M711760), Shuimu Tsinghua Scholar Program (Grant No. 2021SM130), the UK Faraday Institution BESAFE project (FIRG038), and the Imperial College President's PhD Scholarship Scheme (funded by EPSRC). For the purpose of open access, the authors have applied a 'Creative Commons Attribution (CC BY) licence (where permitted by UKRI, 'Open Government Licence' or 'Creative Commons Attribution No-derivatives (CC BY-ND) licence' may be stated instead) to any Author Accepted Manuscript version arising.

Appendix A. Supplementary data

Supplementary data to this article can be found online at https://doi.org/10.1016/j.jpowsour.2023.233926.

References

[1] Y. Liu, Y. Zhu, Y. Cui, Challenges and opportunities towards fast-charging battery materials, Nat. Energy 4 (2019), https://doi.org/10.1038/s41560-019-0405-3.
[2] W. Xie, X. Liu, R. He, Y. Li, X. Gao, X. Li, Z. Peng, S. Feng, X. Feng, S. Yang, Challenges and opportunities toward fast-charging of lithium-ion batteries, J. Energy Storage 32 (2020), 101837, https://doi.org/10.1016/j.est.2020.101837.
[3] W. Xie, R. He, X. Gao, X. Li, H. Wang, X. Liu, X. Yan, S. Yang, Degradation identification of LiNi0.8Co0.1Mn0.1O2/graphite lithium-ion batteries under fast charging conditions, Electrochim. Acta 392 (2021), 138979, https://doi.org/10.1016/j.electacta.2021.138979.
[4] G. Zhang, X. Wei, S. Chen, J. Zhu, G. Han, X. Wang, H. Dai, Revealing the impact of fast charge cycling on the thermal safety of lithium-ion batteries, ACS Appl. Energy Mater. 5 (2022) 7056.
[5] Y. Liu, Y. Zhu, Y. Cui, Challenges and opportunities towards fast-charging battery materials, Nat. Energy 4 (2019) 540–550, https://doi.org/10.1038/s41560-019-0405-3.
[6] A. Tomaszewska, Z. Chu, X. Feng, S. O'Kane, X. Liu, J. Chen, C. Ji, E. Endler, R. Li, L. Liu, Y. Li, S. Zheng, S. Vetterlein, M. Gao, J. Du, M. Parkes, M. Ouyang, M. Marinescu, G. Offer, B. Wu, Lithium-ion battery fast charging: a review, ETransportation 1 (2019), 100011, https://doi.org/10.1016/j.etran.2019.100011.
[7] X. Yue, J. Zhang, Y. Dong, Y. Chen, Z. Shi, X. Xu, X. Li, Z. Liang, Reversible Li plating on graphite anodes through electrolyte engineering for fast-charging batteries, Angew. Chem. Int. Ed. 62 (2023), e202302285, https://doi.org/10.1002/ANIE.202302285.
[8] X. Xu, X. Yue, Y. Chen, Z. Liang, Li plating regulation on fast-charging graphite anodes by a triglyme-LiNO3 synergistic electrolyte additive, Angew. Chem. Int. Ed. 62 (2023), e202306963, https://doi.org/10.1002/ANIE.202306963.
[9] B. Diaz, A. Tomaszewska, M.W. Marzook, K.N. Radhakrishnan, H. Wang, Y. Patel, B. Wu, Lithium ion battery degradation: what you need to know, Phys. Chem. Chem. Phys. 19 (2021), https://doi.org/10.1039/D1CP00359C.
[10] A.S. Mussa, A. Liivat, F. Marzano, M. Klett, B. Philippe, C. Tengstedt, G. Lindbergh, K. Edström, R.W. Lindström, P. Svens, Fast-charging effects on ageing for energy-optimized automotive LiNi1/3Mn1/3Co1/3O2/graphite prismatic lithium-ion cells, J. Power Sources 422 (2019) 175–184, https://doi.org/10.1016/J.JPOWSOUR.2019.02.095.
[11] Y. Chen, L. Torres-Castro, K.H. Chen, D. Penley, J. Lamb, M. Karulkar, N. P. Dasgupta, Operando detection of Li plating during fast charging of Li-ion batteries using incremental capacity analysis, J. Power Sources 539 (2022), 231601, https://doi.org/10.1016/J.JPOWSOUR.2022.231601.
[12] L. Xu, Y. Xiao, Y. Yang, S.J. Yang, X.R. Chen, R. Xu, Y.X. Yao, W.L. Cai, C. Yan, J. Q. Huang, Q. Zhang, Operando quantified lithium plating determination enabled by dynamic capacitance measurement in working Li-ion batteries, Angew. Chem., Int. Ed. 61 (2022), https://doi.org/10.1002/anie.202210365.
[13] D. Ren, H. Hsu, R. Li, X. Feng, D. Guo, X. Han, L. Lu, X. He, S. Gao, J. Hou, Y. Li, Y. Wang, M. Ouyang, A comparative investigation of aging effects on thermal runaway behavior of lithium-ion batteries, ETransportation 2 (2019), 100034, https://doi.org/10.1016/j.etran.2019.100034.
[14] A. Hu, W. Chen, X. Du, Y. Hu, T. Lei, H. Wang, L. Xue, Y. Li, H. Sun, Y. Yan, J. Long, C. Shu, J. Zhu, B. Li, X. Wang, J. Xiong, An artificial hybrid interphase for an ultrahigh-rate and practical lithium metal anode, Energy Environ. Sci. 14 (2021) 4115–4124, https://doi.org/10.1039/D1EE00508A.
[15] A. Hu, F. Li, W. Chen, T. Lei, Y. Li, Y. Fan, M. He, F. Wang, M. Zhou, Y. Hu, Y. Yan, B. Chen, J. Zhu, J. Long, X. Wang, J. Xiong, Ion transport kinetics in low-temperature lithium metal batteries, Adv. Energy Mater. 12 (2022), 2202432, https://doi.org/10.1002/AENM.202202432.
[16] A. Hu, W. Chen, F. Li, M. He, D. Chen, Y. Li, J. Zhu, Y. Yan, J. Long, Y. Hu, T. Lei, B. Li, X. Wang, J. Xiong, Nonflammable polyfluorides-anchored quasi-solid electrolytes for ultra-safe anode-free lithium pouch cells without thermal runaway, Adv. Mater. (2023), 2304762, https://doi.org/10.1002/ADMA.202304762.
[17] X. Feng, D. Ren, X. He, M. Ouyang, Mitigating thermal runaway of lithium-ion batteries, Joule 4 (2020) 743–770, https://doi.org/10.1016/j.joule.2020.02.010.
[18] Y. Li, X. Gao, X. Feng, X. Han, J. Du, L. Lu, M. Ouyang, Parameter-independent error correction for potential measurements by reference electrode in lithium-ion batteries, J. Energy Chem. 67 (2022) 34–45, https://doi.org/10.1016/j.jechem.2021.09.006.
[19] S. Yang, X. Gao, Y. Li, W. Xie, B. Guo, L. Zhang, X. Liu, Minimum lithium plating overpotential control based charging strategy for parallel battery module prevents side reactions, J. Power Sources 494 (2021), 229772, https://doi.org/10.1016/j.jpowsour.2021.229772.
[20] Y. Li, X. Feng, D. Ren, M. Ouyang, L. Lu, X. Han, Thermal runaway triggered by plated lithium on the anode after fast charging, ACS Appl. Mater. Interfaces 11 (2019) 46839–46850, https://doi.org/10.1021/acsami.9b16589.
[21] Y. Li, X. Gao, X. Feng, D. Ren, Y. Li, J. Hou, Y. Wu, J. Du, L. Lu, M. Ouyang, Battery eruption triggered by plated lithium on an anode during thermal runaway after fast charging, Energy 239 (2022), 122097, https://doi.org/10.1016/j.energy.2021.122097.
[22] D. Juarez-Robles, J.A. Jeevarajan, P.P. Mukherjee, Degradation-safety analytics in lithium-ion cells: Part I. Aging under charge/discharge cycling, J. Electrochem. Soc. 167 (2020), 160510, https://doi.org/10.1149/1945-7111/abc8c0.
[23] D. Juarez-Robles, S. Azam, J.A. Jeevarajan, P.P. Mukherjee, Degradation-safety analytics in lithium-ion cells and modules Part II. Overcharge and external short circuit scenarios, J. Electrochem. Soc. 168 (2021), 050535, https://doi.org/10.1149/1945-7111/ac001f.
[24] D. Juarez-Robles, S. Azam, J.A. Jeevarajan, P.P. Mukherjee, Degradation-safety analytics in lithium-ion cells and modules: Part III. Aging and safety of pouch format cells, J. Electrochem. Soc. 168 (2021), 110501, https://doi.org/10.1149/1945-7111/ac30af.
[25] T. Waldmann, M. Wohlfahrt-Mehrens, Effects of rest time after Li plating on safety behavior—ARC tests with commercial high-energy 18650 Li-ion cells, Electrochim. Acta 230 (2017) 454–460, https://doi.org/10.1016/J.ELECTACTA.2017.02.036.
[26] B. Michalak, B.B. Berkes, H. Sommer, T. Brezesinski, J. Janek, Electrochemical cross-talk leading to gas evolution and capacity fade in LiNi0.5Mn1.5O4/graphite full-cells, J. Phys. Chem. C 121 (2017) 211–216, https://doi.org/10.1021/acs.jpcc.6b11184.
[27] D. Lu, S. Lin, W. Cui, S. Hu, Z. Zhang, W. Peng, Swelling mechanism of 0%SOC lithium iron phosphate battery at high temperature storage, J. Energy Storage 32 (2020), 101791, https://doi.org/10.1016/j.est.2020.101791.
[28] K.Y. Oh, B.I. Epureanu, J.B. Siegel, A.G. Stefanopoulou, Phenomenological force and swelling models for rechargeable lithium-ion battery cells, J. Power Sources 310 (2016) 118–129, https://doi.org/10.1016/j.jpowsour.2016.01.103.
[29] S. Wang, J. Liu, K. Rafiz, Y. Jin, Y. Li, Y.S. Lin, An on-line transient study on gassing mechanism of lithium titanate batteries, J. Electrochem. Soc. 166 (2019) A4150–A4157, https://doi.org/10.1149/2.0631916jes.
[30] U. Mattinen, M. Klett, G. Lindbergh, R. Wreland Lindström, Gas evolution in commercial Li-ion battery cells measured by on-line mass spectrometry – effects of C-rate and cell voltage, J. Power Sources 477 (2020), 228968, https://doi.org/10.1016/J.JPOWSOUR.2020.228968.
[31] A. Devie, M. Dubarry, H.-P. Wu, T.-H. Wu, B.Y. Liaw, Overcharge study in Li4Ti5O12 based lithium-ion pouch cell, J. Electrochem. Soc. 163 (2016) A2611, https://doi.org/10.1149/2.0491613JES.
[32] D. Ren, X. Feng, L. Lu, X. He, M. Ouyang, Overcharge behaviors and failure mechanism of lithium-ion batteries under different test conditions, Appl. Energy 250 (2019) 323–332, https://doi.org/10.1016/j.apenergy.2019.05.015.
[33] R. Gordon, A. Smith, Towards more realistic Li-ion battery safety tests based on Li-plating as internal cell error, J. Energy Storage 72 (2023), https://doi.org/10.1016/j.est.2023.108200, 2352–152.
[34] X. Feng, M. Fang, X. He, M. Ouyang, L. Lu, H. Wang, M. Zhang, Thermal runaway features of large format prismatic lithium ion battery using extended volume

accelerating rate calorimetry, J. Power Sources 255 (2014) 294–301, https://doi.org/10.1016/j.jpowsour.2014.01.005.
[35] G. Wang, D. Kong, P. Ping, J. Wen, X. He, H. Zhao, X. He, R. Peng, Y. Zhang, X. Dai, Revealing particle venting of lithium-ion batteries during thermal runaway: a multi-scale model toward multiphase process, ETransportation 16 (2023), 100237, https://doi.org/10.1016/J.ETRAN.2023.100237.
[36] X. Gao, Xi Liu, W. Xie, L. Zhang, S. Yang, Multiscale observation of Li plating for lithium-ion batteries, Rare Met. 40 (2021) 3038–3048, https://doi.org/10.1007/s12598-021-01730-3.
[37] X.G. Yang, S. Ge, T. Liu, Y. Leng, C.Y. Wang, A look into the voltage plateau signal for detection and quantification of lithium plating in lithium-ion cells, J. Power Sources 395 (2018) 251–261, https://doi.org/10.1016/j.jpowsour.2018.05.073.
[38] D. Ren, K. Smith, D. Guo, X. Han, X. Feng, L. Lu, M. Ouyang, J. Li, Investigation of lithium plating-stripping process in Li-ion batteries at low temperature using an electrochemical model, J. Electrochem. Soc. 165 (2018) A2167, https://doi.org/10.1149/2.0661810jes. A2167.
[39] P. Liu, L. Yang, B. Xiao, H. Wang, L. Li, S. Ye, Y. Li, X. Ren, X. Ouyang, J. Hu, F. Pan, Q. Zhang, J. Liu, Revealing lithium battery gas generation for safer practical applications, Adv. Funct. Mater. 32 (2022), https://doi.org/10.1002/adfm.202208586.
[40] C. Sångeland, J. Mindemark, R. Younesi, D. Brandell, Probing the interfacial chemistry of solid-state lithium batteries, Solid State Ionics 343 (2019), 115068, https://doi.org/10.1016/j.ssi.2019.115068.
[41] X.-G. Yang, T. Liu, Y. Gao, S. Ge, Y. Leng, D. Wang, C.-Y. Wang, Asymmetric temperature modulation for extreme fast charging of lithium-ion batteries, Joule 3 (2019) P3002, https://doi.org/10.1016/j.joule.2019.09.021.
[42] Y. Wang, D. Ren, X. Feng, L. Wang, M. Ouyang, Thermal kinetics comparison of delithiated Li $[Ni_xCo_yMn_{1-x-y}]O_2$ cathodes, J. Power Sources 514 (2021), 230582, https://doi.org/10.1016/j.jpowsour.2021.230582.
[43] Y. Wang, X. Feng, W. Huang, X. He, L. Wang, M. Ouyang, Challenges and opportunities to mitigate the catastrophic thermal runaway of high-energy batteries, Adv. Energy Mater. 2203841 (2023) 1–27, https://doi.org/10.1002/aenm.202203841.
[44] X. Liu, D. Ren, H. Hsu, X. Feng, G.L. Xu, M. Zhuang, H. Gao, L. Lu, X. Han, Z. Chu, J. Li, X. He, K. Amine, M. Ouyang, Thermal runaway of lithium-ion batteries without internal short circuit, Joule 2 (2018) 2047–2064, https://doi.org/10.1016/J.JOULE.2018.06.015.
[45] Y. Wang, X. Feng, Y. Peng, F. Zhang, D. Ren, X. Liu, L. Lu, Y. Nitta, L. Wang, M. Ouyang, Reductive gas manipulation at early self-heating stage enables controllable battery thermal failure, Joule 6 (2022) 2810–2820, https://doi.org/10.1016/j.joule.2022.10.010.